Use of Helper Enzymes for ADP Removal in Infrared Spectroscopic Experiments: Application to Ca^{2+}-ATPase

Man Liu, Eeva-Liisa Karjalainen, and Andreas Barth
Department of Biochemistry and Biophysics, The Arrhenius Laboratories for Natural Sciences, Stockholm University, S-106 91 Stockholm, Sweden

ABSTRACT Adenylate kinase (AdK) and apyrase were employed as helper enzymes to remove ADP in infrared spectroscopic experiments that study the sarcoplasmic reticulum Ca^{2+}-ATPase. The infrared absorbance changes of their enzymatic reactions were characterized and used to monitor enzyme activity. AdK transforms ADP to ATP and AMP, whereas apyrase consumes ATP and ADP to generate AMP and inorganic phosphate. The benefits of using them as helper enzymes are severalfold: i), both remove ADP generated after ATP hydrolysis by ATPase, which enables repeat of ATP-release experiments several times with the same sample without interference by ADP; ii), AdK helps maintain the presence of ATP for a longer time by regenerating 50% of the initial ATP; iii), apyrase generates free P_i, which can help stabilize the ADP-insensitive phosphoenzyme (E2P); and iv), apyrase can be used to monitor ADP dissociation from transient enzyme intermediates with relatively high affinity to ADP, as shown here for ADP dissociation from the ADP-sensitive phosphoenzyme intermediate (Ca_2E1P). The respective infrared spectra indicate that ADP dissociation relaxes the closed conformation immediately after phosphorylation partially back toward the open conformation of Ca_2E1 but does not trigger the transition to E2P. The helper enzyme approach can be extended to study other nucleotide-dependent proteins.

INTRODUCTION

Use of caged nucleotides (Kaplan et al., 1978) is one approach in infrared spectroscopy (Barth et al., 1990, 1996; Buchet et al., 1991; Cepus et al., 1998a; Du et al., 2000; Raimbault et al., 1996; Troullier et al., 1996; von Germar et al., 1999) to trigger reactions between an enzyme and nucleotides directly in an infrared cuvette, as previously reviewed (Barth and Zscherp, 2000, 2002; Cepus et al., 1998b; Mäntele, 1993, 1996; Siebert, 1995). After a nucleoside triphosphate is hydrolyzed by an enzyme, a nucleoside diphosphate is generated that one may want to remove. Adenylate kinase (AdK) and apyrase are suitable to achieve this aim. We studied their use in infrared spectroscopic experiments and characterized the difference spectra of their enzymatic reactions. They were applied to investigate the sarcoplasmic reticulum Ca^{2+}-ATPase (SERCA1a). This ATPase transports Ca^{2+} ions actively against a concentration gradient with energy derived from ATP (Hasselbach and Makinose, 1961; Lee and East, 2001; MacLennan and Green, 2000; Martonosi and Pikula, 2003; Stokes and Green, 2003; Toyoshima and Inesi, 2004).

In the reaction cycle of Ca^{2+} transfer (Scheme 1), the ATPase undergoes conformational changes and forms several intermediates including Ca_2E1 (the calcium-ATPase complex with high affinity to Ca^{2+}), Ca_2E1ATP (the calcium-ATP-ATPase complex), Ca_2E1P (the ADP-sensitive phosphoenzyme), E2P (the ADP-insensitive phosphoenzyme), and E2 (the calcium-free ATPase with low affinity to Ca^{2+}).

Upon ATP hydrolysis by the ATPase, ADP is formed and binds to the ATPase at the end of measurements (Barth et al., 1994), which inhibits the binding of ATP released in subsequent ATP-release experiments. This makes it unsuitable to repeat the experiment with the same sample. With helper enzymes that remove ADP, one can repeat experiments with the same sample. This is a more efficient way of averaging a given number of experiments and saves time and sample. It is particularly valuable in infrared spectroscopic experiments which do not allow change of the sample medium since preparation of a new sample and its equilibration takes ~1 h.

AdK is a monomeric enzyme that catalyzes the conversion of adenine nucleotides between ADP and ATP/AMP: $2ADP \rightleftharpoons ATP + AMP$ (Atkinson, 1968), which is used in ATP regenerating systems (see for example the review by Whitesides et al., 1976). *Escherichia coli* AdK shows a broad specificity for nucleotides, with the highest preference toward UDP for UTP synthesis (Lu and Lnouye, 1996). AdK also converts 2′-dADP (Ladner and Whitesides, 1985; Resnick and Zehnder, 2000), with a lower efficiency compared to ADP (Ladner and Whitesides, 1985; Liu and Barth, 2004).

Potato apyrase is a monomeric enzyme that liberates inorganic phosphate from tri- and diphosphate nucleosides in the presence of divalent cations (Mg^{2+} or Ca^{2+}; Kalckar, 1944; Komosyznski and Wojtczak, 1996; Meyerhof, 1945), for example from ATP and ADP: $ATP \rightarrow ADP + P_i \rightarrow AMP + 2P_i$. Potato apyrase can also split inosine tri- and diphosphate (ITP and IDP) with half of the rate found for ATP and ADP (Kalckar, 1944). It is used to remove ADP

Submitted November 1, 2004, and accepted for publication February 8, 2005.

Address reprint requests to Andreas Barth, Dept. of Biochemistry and Biophysics, The Arrhenius Laboratories for Natural Sciences, Stockholm University, SE-106 91 Stockholm, Sweden. Tel.: 46-8-162452; Fax: 46-8-155597; E-mail: Andreas.Barth@dbb.su.se.

0006-3495/05/05/3615/10 $2.00

doi: 10.1529/biophysj.104.055368

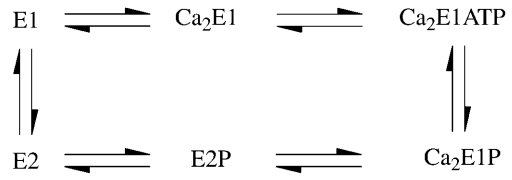

SCHEME 1 Simplified scheme of the Ca^{2+}-ATPase reaction cycle.

(Plow and Marguerie, 1980; West et al., 1967) and ATP (Straub and Feuer, 1950).

MATERIALS AND METHODS

Infrared samples were prepared by drying the sample solution on a CaF_2 window with a trough of 5-μm depth and 8-mm diameter. The samples were immediately rehydrated with ~0.5 μl H_2O and sealed with a second flat CaF_2 window. The approximate composition of samples without the Ca^{2+}-ATPase based on a 1-μl sample volume is 10 mM $CaCl_2$, 10 mM DTT, 1 mg/ml AdK or 2-5 mg/ml apyrase, 10 mM caged ADP or caged ATP [P^3-1-(2-nitrophenyl)ethyl ADP or ATP], 150 mM methylimidazole (pH 7.5), and 150 mM KCl. In the samples with Ca^{2+}-ATPase, there are also 1.2 mM Ca^{2+}-ATPase and 0.5 mg/ml Ca^{2+} ionophore (A23187). Each experiment was repeated three to eight times with at least two different samples (one to four flashes applied to one sample). Samples with 500 mM ATP, ADP, or AMP dissolved in 2000 mM KOH, or with 500 mM AMP and 1000 mM K_2HPO_4 dissolved in 2000 mM KOH, were prepared to record absorption spectra with BaF_2 windows (10–30 μm path length).

AdK (M5520) and apyrase (A6535) were purchased from Sigma (St. Louis, MO). Caged compounds were synthesized by J. E. T. Corrie at the National Institute of Medical Research, London.

FTIR measurements

Time-resolved Fourier transform infrared (FTIR) measurements were performed at 1°C with a Bruker IFS 66/S spectrometer as described (Barth et al., 1996; Liu and Barth, 2003b). Photolytic release of ATP or ADP from the respective caged derivatives was triggered by a Xenon flash tube (N-185C; Xenon Corporation, Woburn, MA). Spectra were recorded in the following way: 1), a reference spectrum was first recorded; and 2), after applying the photolysis flash, a time-resolved infrared spectra with 65 ms time resolution was recorded. Difference spectra were obtained by subtracting the reference spectrum from the spectra recorded after photolytic release of ATP or ADP. They reflect absorbance changes due to reactions of AdK or apyrase with ATP and/or ADP, and of the Ca^{2+}-ATPase if present, as well as the photolysis reaction. Groups or structures not involved in the reactions do not manifest in the difference spectra.

Model spectra

Model spectra for the enzymatic reactions were obtained from different combinations of absorption spectra: i), for AdK: ATP spectrum + AMP spectrum − 2 × ADP spectrum (ATP + AMP − 2ADP); and ii), for apyrase: (AMP + P_i) spectrum − ADP spectrum, and (AMP + 2P_i) spectrum − ATP spectrum.

Kinetic evaluation of reactions

Time courses of the reactions were obtained by fitting the integrated area of selected difference bands corresponding to ATP/AMP formation and ADP consumption in AdK experiments to ATP/ADP splitting and to AMP and inorganic phosphate generation in apyrase experiments, as discussed below. We selected bands for integration by comparison of model spectra and difference spectra obtained from AdK or apyrase experiments. Bands were integrated with respect to a baseline drawn between two points at both sides of the bands with method ''E'' of OPUS 4.0 as described (Barth et al., 1996; Barth and Mäntele, 1998; Liu and Barth, 2003b).

RESULTS

AdK reaction with ADP

Photolysis of caged ADP and subsequent reactions were monitored by time-resolved FTIR spectroscopy in the absence and the presence of AdK. Because there is nearly no difference of absorption between ATP, ADP, and AMP above 1300 cm^{-1}, we only show the spectra between 1350 and 900 cm^{-1} where phosphate groups dominate the absorption because of their high extinction coefficient. AdK concentration was too low to detect absorbance changes of AdK in the entire spectral range from 1800 to 900 cm^{-1}.

Fig. 1 shows a model spectrum of the AdK reaction with ADP (ATP + AMP − 2 ADP) and difference spectra after ADP release in the absence or presence of AdK. Spectra of ATP, ADP, and AMP (Brintzinger, 1965; Epp et al., 1958; Takeuchi et al., 1988), GDP (Wang et al., 1998), monomethyl diphosphate (model for ADP; Brintzinger, 1965), and monomethyl phosphate (model for AMP; Brintzinger, 1965; Shimanouchi et al., 1964) have been published previously. In the model spectrum, positive bands show the absorption of ATP and AMP, negative bands the absorption of ADP. In the presence of AdK, absorbance changes were observed between 10 and 81 s due to the formation of AMP and ATP from ADP (*bold* spectrum in Fig. 1). As expected, no significant absorbance difference was observed in the absence of AdK in the same time interval after the photolysis flash (*shaded* spectrum in Fig. 1). Photolysis signals do not contribute to the spectra because photolysis is complete in the first spectrum used to generate the difference spectra.

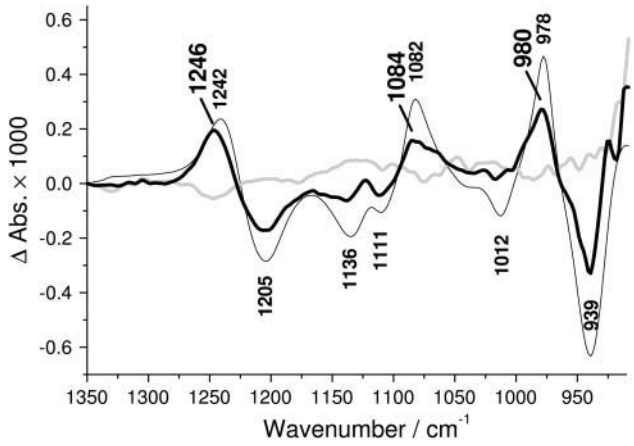

FIGURE 1 Spectra of the AdK reaction to generate ATP and AMP from ADP. (*Shaded line* and *bold line*) The difference spectrum obtained with 3 mM ADP released from caged ADP in the absence and in the presence of 1 mg/ml AdK, respectively, calculated by subtracting the spectrum recorded at 10 s from that at 81 s after the photolysis flash; thin line, a model spectrum of the AdK reaction calculated with absorption spectra: ATP + AMP − 2 ADP.

By comparing the spectrum obtained in the presence of AdK with the model spectrum and absorption spectra (data not shown), the bands at 1246 and 1084 cm^{-1} can be assigned to ATP, those at 1205, 1136, and 939 cm^{-1} to ADP, and that at 980 cm^{-1} predominantly to AMP. These bands were used to evaluate the time course of the AdK reaction. Time courses of the bands are shown in Fig. 2. Data were measured from 0 to 240 s. The integrated band areas remain constant after 125 s. Here we show the data until 150 s.

The area of the 1205 cm^{-1} band increased initially, due to an overlapping band between 1200 and 1180 cm^{-1} from photolysis of caged ADP (Barth et al., 1994). The following decrease of the band area indicates ADP consumption due to the AdK reaction. The band areas at 980 and 1246 cm^{-1} first decreased to a minimum and then increased until they reached plateaus. The decrease is due to photolysis of caged ADP (Barth et al., 1994), which absorbs at similar positions as AMP and ATP do. The increase of band areas is induced by the formation of AMP and ATP, which absorb at 980 and 1246 cm^{-1}, respectively. By fitting the band areas with second order exponential decay functions, we obtained two time constants (Fig. 2). The fast absorbance changes are due to photolysis of caged ADP. The respective time constants obtained from the fits are 0.1–0.6 s. They do not reflect accurate measurements of the photolysis rate because of only four data points in the first 2 s. The slow time constant is ~32 s, reflecting the AdK reaction of ADP conversion to ATP and AMP.

AdK reaction with ADP in the presence of the Ca^{2+}-ATPase

To demonstrate that AdK can alter the nucleotide composition of the ATPase samples and affect ATPase partial reactions, ADP release in Ca^{2+}-ATPase samples was monitored in the absence and the presence of AdK.

In the absence of AdK, we observed infrared absorbance changes induced by ADP release from caged ADP and ADP binding to the ATPase, which are shown in Fig. 3 (*shaded* spectrum). The spectrum exhibits a similar spectral shape but smaller band amplitudes in the amide I region compared to the ATP binding spectrum (Barth et al., 1996; Liu and Barth, 2003a; von Germar et al., 2000). The latter is partly due to the missing γ-phosphate and partly due to incomplete binding to the ATPase under the conditions used here (only 3 mM ADP released). No further absorbance changes were observed after ~3 s in our measurement (total time of measurement: 240 s). The bands in the amide I region (1700–1610 cm^{-1}) indicate conformational changes of the ATPase backbone upon ADP binding (Barth et al., 1994). The band at 1628 cm^{-1} is a marker band for nucleotide binding to Ca_2E1 (Barth et al., 1996; Liu and Barth, 2002, 2003a) and has been tentatively assigned (Liu and Barth, 2004) to a conformational change in the β-sheet of the phosphorylation domain (Toyoshima et al., 2000) of the ATPase. The negative band at 1525 cm^{-1} is a photolysis band, assigned to the antisymmetric stretching vibration of the nitro group of caged ADP (Barth et al., 1990, 1995).

In the presence of AdK, the reactions occurring in the samples are more diverse and include ADP release from caged ADP, ADP binding to the Ca^{2+}-ATPase (Ca_2E1ADP), ADP conversion to ATP and AMP by AdK, binding of generated ATP to the ATPase, ATP hydrolysis to ADP and ATPase phosphorylation (Ca_2E1P), removal of ADP generated from ATP hydrolysis, etc. In our time-resolved FTIR measurements, we first observed the spectrum of ADP binding to the ATPase (spectrum *I* in Fig. 3), showing similar band positions and amplitudes as that

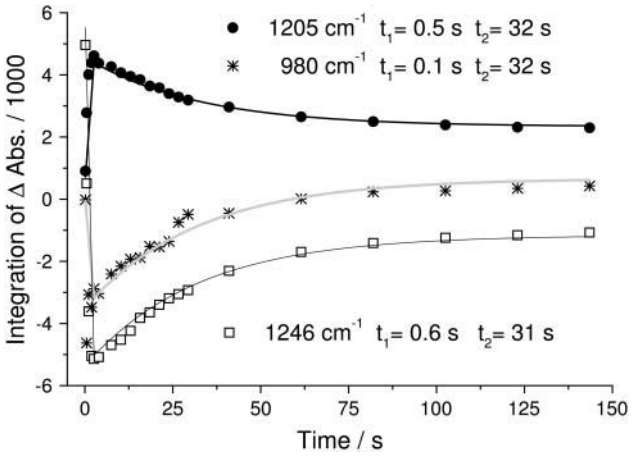

FIGURE 2 Kinetics of the AdK reaction with ADP, shown with integrated band intensities at 1246 cm^{-1} for ATP formation, at 1205 cm^{-1} for ADP consumption, and at 980 cm^{-1} for AMP formation, obtained with ~3 mM released ADP and 1 mg/ml AdK. Time constants and lines were obtained by fitting data with second order exponential functions.

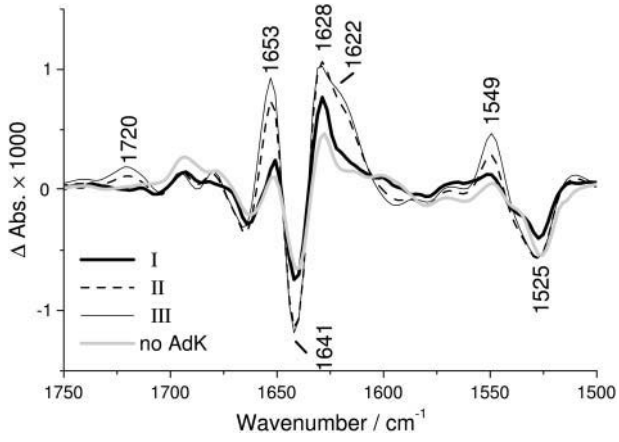

FIGURE 3 Difference spectra of ADP release (3 mM) in ATPase (~1.2 mM) samples in the presence and absence of 1 mg/ml AdK (1°C, pH 7.5). Spectra I, II, and III obtained in the presence of AdK were averaged in the time intervals 0.34–0.67 s, 14.4–30.7 s, and 174–236 s after ADP release. The shaded spectrum is the spectrum of ADP binding (3 mM ADP) averaged in the time interval 0.46–3.24 s obtained in the absence of AdK.

obtained in the absence of AdK (the *shaded* spectrum in Fig. 3). In the spectra recorded later (spectrum *II* and *III* in Fig. 3) the marker bands of ATPase phosphorylation were observed at 1720 and 1549 cm^{-1}, as well as the shoulder at 1622 cm^{-1} characteristic of ATP binding and the first phosphorylated enzyme intermediate Ca_2E1P (Barth and Mäntele, 1998; Liu and Barth, 2003a). This experiment demonstrated that in the presence of AdK, a portion of ADP molecules bound initially to the ATPase, whereas AdK generated ATP and AMP from the remaining portion. ATP then replaced ADP in the binding site of ATPase and phosphorylated the ATPase. In consequence, the marker bands of phosphorylation were observed, as shown in spectrum II and III of Fig. 3. Meanwhile, band amplitudes in the amide I region increased during the measurements because of the conformational changes that were induced by ATP binding to the ATPase and ATPase phosphorylation (Barth et al., 1996; Liu and Barth, 2003a, 2004).

Kinetics of the AdK reaction in the presence of the Ca^{2+}-ATPase

Kinetic changes of some marker band areas are shown in Fig. 4: those of bands at 1720 and 1549 cm^{-1} for ATPase phosphorylation, at 1628 cm^{-1} for ATP and ADP binding to the Ca^{2+} bound form Ca_2E1 and Ca_2E1P, at 1622 cm^{-1} for ATP binding to Ca_2E1P, at 1212 cm^{-1} for ADP release and its consumption by AdK, and at 980 cm^{-1} for AMP formation by AdK. Since ATP is produced concomitantly with AMP, the latter band also indirectly monitors ATP production.

The time course of the bands at 1212 cm^{-1} has to be fitted with two time constants. The first time constant (~0.5 s) indicates photolysis of caged ADP and is similar to that observed in the absence of ATPase. The second time constant is 17 s, indicating ADP consumption, and is similar to the time constant of AMP formation observed at 980 cm^{-1} (20 s). The AdK reaction is faster in the presence than in the absence of ATPase (~32 s). This is probably because the ATPase inhibits the AdK back reaction with ATP and AMP by binding the reaction product ATP and regenerating ADP.

The apparent time constant of ATPase phosphorylation is ~17 s, obtained by kinetic evaluation of the band areas at 1720 and 1549 cm^{-1}. The kinetic change of band areas at 1628 (for nucleotide binding to Ca_2E1 and Ca_2E1P, respectively) was fitted with one time constant (1 s) and that at 1622 cm^{-1} with two time constants (0.5 and 13 s). The fast phase corresponds to ADP binding to Ca_2E1. This is consistent with that observed in the absence of AdK (data not shown) and is rate limited by photolysis of caged ADP (Barth et al., 1996; Liu and Barth, 2003a). The second time constant of ~13 s accounts for the slow increase of absorbance changes due to ATP binding to the ATPase and ATPase phosphorylation. This time constant coincides with the time constant of the AdK reaction. The kinetics of ATP binding and ATPase phosphorylation are only revealed at 1622 cm^{-1}

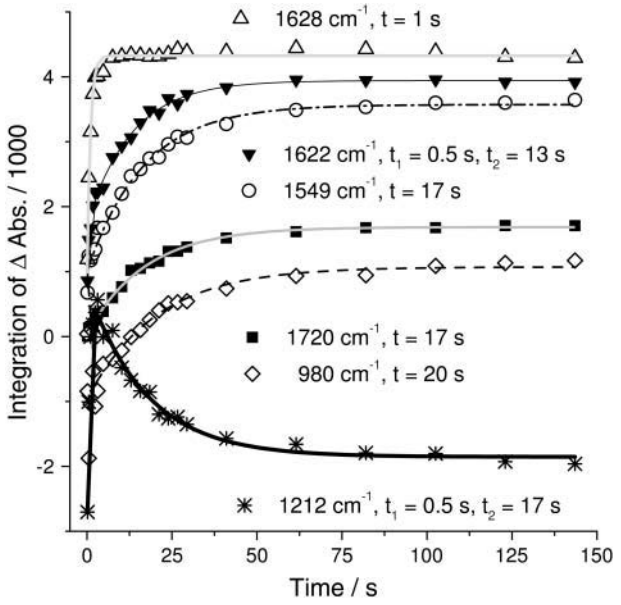

FIGURE 4 Time courses of selected infrared bands upon release of 3 mM ADP in ATPase (1.2 mM) samples containing 1 mg/ml AdK, at 1622 cm^{-1} for ATP binding to the ATPase, at 1628 cm^{-1} for ADP and ATP binding to the ATPase, at 1720 and 1549 cm^{-1} for ATPase phosphorylation, at 1212 cm^{-1} for ADP release and consumption, and at 980 cm^{-1} for AMP formation (1°C, pH 7.5). Time constants and lines were obtained by fitting data with first or second order exponential functions.

where a shoulder appears that is not observed upon ADP binding (compare *bold* and *thin line* spectra in Fig. 3).

Upon release of 3 mM ATP, the time constants of ATP binding to the ATPase and ATPase phosphorylation are ~0.1 s and ~2 s, respectively, obtained in the absence and the presence of AdK (Liu and Barth, 2003a, 2004). Both are smaller than the 13–17 s observed here. This indicates that ATP generation from ADP in the AdK reaction is rate limiting compared to ATP binding and ATPase phosphorylation.

Apyrase reactions with ADP and ATP

Apyrase hydrolyzes ATP to ADP and P_i, and ADP to AMP and P_i. Fig. 5 shows the difference spectra of ADP or ATP splitting by apyrase (*bold* spectra) and model spectra (*thin* spectra) calculated with absorption spectra of AMP + $2P_i$, AMP + P_i, ADP, and ATP.

In the upper panel of Fig. 5, the difference spectrum of the reaction of ADP with apyrase is consistent with the model spectrum of AMP + P_i − ADP. From the absorption spectra, we assign the negative bands at 1213, 1137, and 939 cm^{-1} to ADP, the positive band at 1082 cm^{-1} to AMP and P_i, and that at 980 cm^{-1} to AMP. A shoulder near 990 cm^{-1} is characteristic of P_i. The time courses of the integrated band areas at 1213, 1082, and 980 cm^{-1} are shown in Fig. 6. Data fitting suggested an average time constant of 16 s for ADP splitting by apyrase under our conditions.

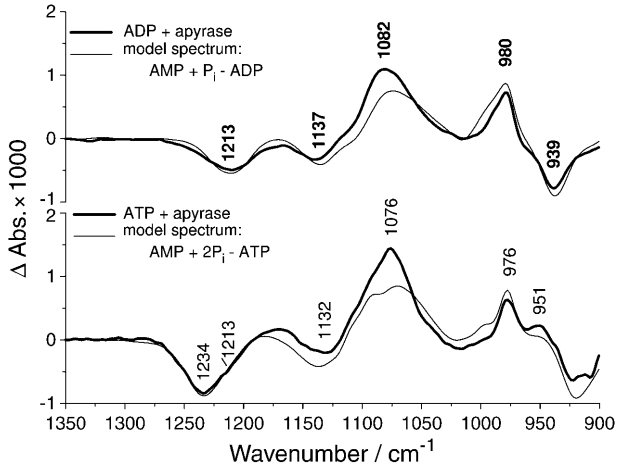

FIGURE 5 Difference spectra of ADP or ATP splitting by 3 or 5 mg/ml apyrase (10 mM Ca^{2+}, 1°C, pH 7.5), respectively, and model spectra calculated with absorption spectra of AMP + P_i, ADP, AMP + $2P_i$, and ATP. (*Upper panel*) Difference spectrum with labels of band positions obtained with apyrase and ADP, calculated by subtracting the spectrum averaged from 0.96 to 3.4 s after ADP release from that averaged from 174 to 236 s. (*Lower panel*) Difference spectrum with labels of band positions obtained with apyrase and ATP, calculated by subtracting the spectrum averaged from 0.96 to 3.4 s after ATP release from that averaged from 174 to 236 s.

In the lower panel of Fig. 5, the difference spectrum of the reaction of ATP with apyrase is partly consistent with the respective model spectrum of AMP + $2P_i$ − ATP. In the difference spectrum we assign the band at 1234 cm^{-1} to ATP, that at 951 cm^{-1} to ADP, that at 1076 cm^{-1} to predominantly P_i, and that at 976 cm^{-1} to AMP. The small ADP band at 951 cm^{-1} shows that there are still ADP molecules present, which have not been hydrolyzed by apyrase at the end of our measurements.

The time courses of infrared bands were evaluated to obtain time constants for ATP and ADP splitting by apyrase. For the broad 1234 cm^{-1} band, two regions were analyzed to distinguish between ATP and ADP: the region around 1213 cm^{-1} characteristic of ADP, and the high wavenumber side of the 1234 cm^{-1} ATP band around 1241 cm^{-1}, which has no overlap with the ADP band at 1213 cm^{-1}. Kinetic changes of the bands at 1241, 1213, 1076, and 976 cm^{-1} are shown from 0 to 150 s in Fig. 7. Data were measured until 250 s, and the plateaus of integrated band areas were reached after 75 s. Bands at 1241, 1213, and 976 cm^{-1} were fitted with first order exponential functions. The time constant of ATP splitting (1241 cm^{-1}) is 13 s, whereas the time constant of ADP splitting (1213 cm^{-1}) is 25 s. It is within experimental error the same as that of AMP formation at 976 cm^{-1} where the fit gives 32 s. The 1076 cm^{-1} band originates from P_i production upon ATP and ADP splitting. It was therefore fitted with a second order exponential function with fixed time constants for ATP and ADP splitting obtained as described above. (For ADP splitting, the average of the 1213 and 976 cm^{-1} fit results was used: 28 s.) This fit shows that the kinetic change at 1076 cm^{-1} can be explained solely by the two reactions of ADP and ATP splitting. ADP splitting in the presence of ATP is slightly slower than that observed with only ADP and apyrase (16 s; see Fig. 6). This is due to the competition between ATP and ADP (Kalckar, 1944). In our samples the concentration of ADP is lower than that of ATP probably during most of the reaction, which prevents ADP binding to the active site of apyrase (Komosyznski and Wojtczak, 1996). This explains the small band at 951 cm^{-1} in the difference spectrum obtained with ATP and apyrase (*lower panel* of Fig. 5), showing that ADP is not completely hydrolyzed by the end of our measurements.

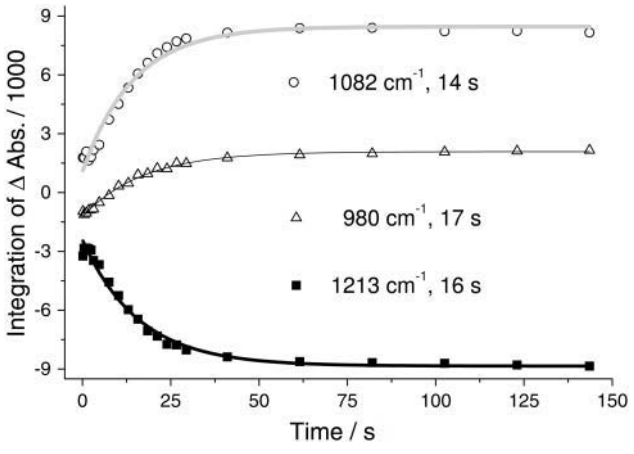

FIGURE 6 Time courses of 3 mM ADP splitting by 3 mg/ml apyrase evaluated with bands at 1213 cm^{-1} for ADP consumption, at 1082 cm^{-1} for P_i formation, and at 980 cm^{-1} for AMP formation (10 mM Ca^{2+}, 1°C, pH 7.5). Time constants and lines were obtained by fitting data with first order exponential functions.

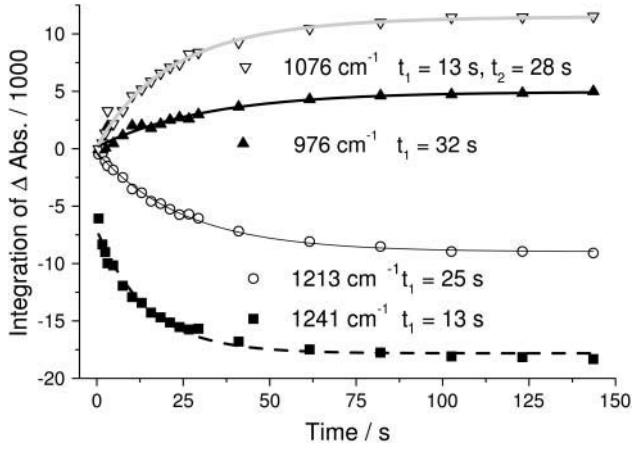

FIGURE 7 Time courses of 3 mM ATP splitting by 5 mg/ml apyrase evaluated with bands at 1241 cm^{-1} for ATP consumption, at 1213 cm^{-1} for ADP consumption, at 1076 cm^{-1} for P_i formation, and at 976 cm^{-1} for AMP formation (10 mM Ca^{2+}, 1°C, pH 7.5). Time constants and lines are calculated by fitting data with first or second order exponential functions.

Experiments shown in Figs. 4–6 of the apyrase reaction with ATP and ADP were done at pH 7.5. At pH 6, which is the optimal pH value for apyrase activity, the reaction is faster, with a time constant of 9 s for the reaction between apyrase and ADP and of 7 s between apyrase and ATP (data not shown).

Apyrase reaction with ADP in the presence of the Ca^{2+}-ATPase

In the presence of the Ca^{2+}-ATPase, 3 mg/ml apyrase is enough to efficiently hydrolyze ADP under our conditions. If more apyrase were present, ADP splitting would be too fast to observe the ADP-ATPase complex Ca_2E1ADP.

Fig. 8 *A* shows the difference spectra averaged in different time intervals obtained in the presence of ADP, apyrase, and ATPase. The first spectrum that averaged from 1.4 to 2.7 s (*shaded* spectrum in Fig. 8 *A*) shows absorbance changes upon ADP binding to the ATPase ($Ca_2E1 \rightarrow Ca_2E1ADP$), which is very similar to the spectrum obtained in the absence of apyrase (*shaded* spectrum in Fig. 3). In the later spectra that were averaged from 6.8 to 20.5 s and from 144 to 246 s, the band amplitudes in the amide I region decrease, indicating a decay of Ca_2E1ADP. This is because ADP molecules were hydrolyzed by apyrase to AMP and P_i. At the end of experiments, absorbance changes remain, which are likely due to photolysis of caged ADP because a band near 1633 cm^{-1} appears in photolysis spectra of caged ADP and caged ATP in methylimidazole buffer in the presence of DTT.

The kinetic change of the marker band area at 1628 cm^{-1} of nucleotide binding is shown in Fig. 8 *B*, demonstrating clearly the effect of apyrase on ADP binding to the ATPase. The band area first increases fast to reach a maximum and then decreases slowly until it reaches a plateau. Data were fitted with two time constants. The fast component (0.2 s) is induced by ADP binding to the Ca^{2+}-ATPase, which is the same as that obtained in the absence of apyrase. The slow component (17 s) indicates dissociation of ADP from the ATPase, which is irreversible due to the consumption of ADP by apyrase. The time constant for ADP dissociation is the same as that of ADP splitting by apyrase obtained in the absence of ATPase, showing that the apyrase reaction is rate limiting under our conditions.

Apyrase reaction with ATP in the presence of the Ca^{2+}-ATPase

The apyrase reaction with ATP was also investigated in the presence of the Ca^{2+}-ATPase. In this case, apyrase was used to remove ADP generated after ATP hydrolysis upon the formation of Ca_2E1P. ADP binds to Ca_2E1P (Inesi et al., 2004; Liu and Barth, 2004), and the addition of apyrase to our samples allowed us to observe ADP dissociation from Ca_2E1P.

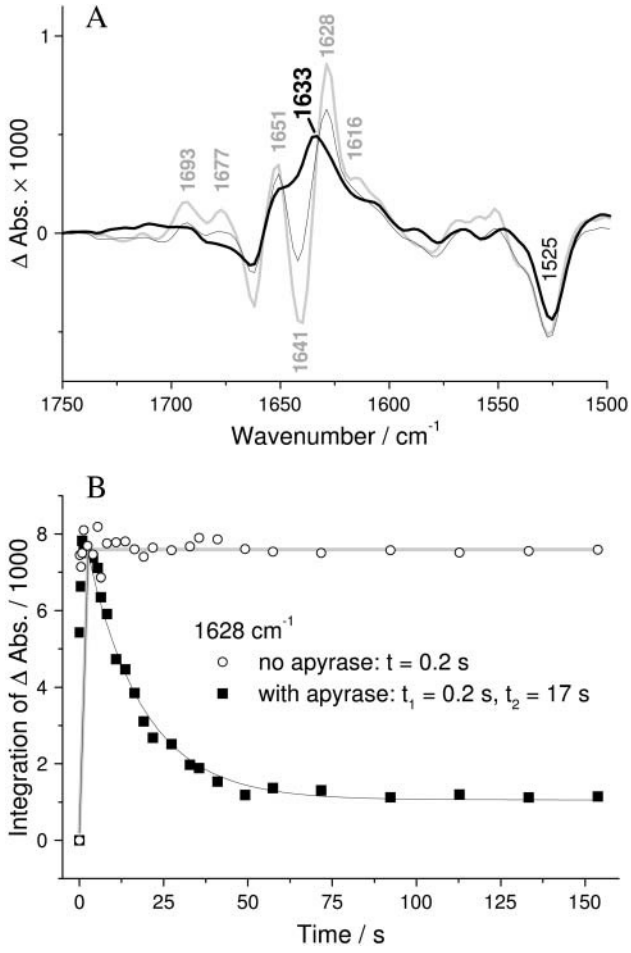

FIGURE 8 (*A*) Infrared difference spectra obtained upon release of 3 mM ADP in samples containing 1.2 mM ATPase and 3 mg/ml apyrase (10 mM Ca^{2+}, 1°C, pH 7.5) in different time intervals: shaded line, 1.4–2.7 s; thin line, 6.8–20.5 s; and bold line, 144–246 s. (*B*) Time courses of the band area at 1628 cm^{-1} in the presence and absence of apyrase. Time constants and lines were obtained by fitting data with second order exponential functions.

In the presence of apyrase and ATPase, we first observed ATP binding (*dotted* spectrum in Fig. 9 *A*) and ATPase phosphorylation (*shaded* spectrum in Fig. 9 *A*) indicated by marker bands at 1720 and 1549 cm^{-1}. The amplitude in the amide I region decreased slightly when the ATPase converted to the Ca_2E1P state, in line with previous observations (Barth and Mäntele, 1998; Liu and Barth, 2003a). In the time range from 5 to ~60 s, the 1720 cm^{-1} band retained the same amplitude, whereas the bands in the amide I region decreased in amplitude (*black* spectrum in Fig. 9 *A*), indicating that the concentration of Ca_2E1P is constant but the conformation of Ca_2E1P changes. This is due to the presence of apyrase; in the absence of apyrase, the bands in the amide I region retain their amplitude until the end of measurements (over 240 s).

The time course of the band area at 1628 cm^{-1} from 0 to 225 s has been discussed before in the absence and presence of apyrase (Liu and Barth, 2004). Here it is shown in Fig. 9

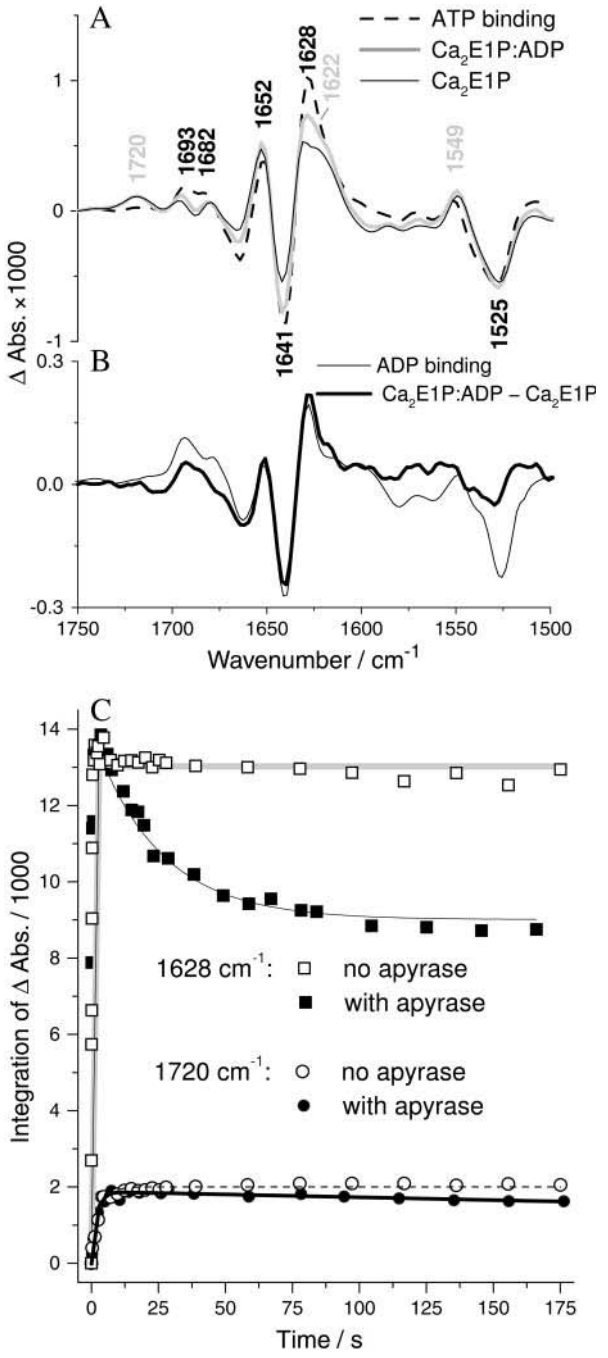

FIGURE 9 (*A*) Infrared difference spectra upon 3 mM ATP release in ATPase (1.2 mM) samples containing 5 mg/ml apyrase (10 mM Ca^{2+}, 1°C, pH 7.5) at different time intervals after ATP release: dotted line, spectrum of ATP binding to Ca_2E1 averaged from 0.3 to 1.1 s; shaded line, the spectrum of Ca_2E1P with ADP bound averaged from 2.7 to 4.1 s; and thin line, the Ca_2E1P spectrum after ADP dissociation averaged from 46.5 to 60 s. (*B*) Comparison of ADP binding to Ca_2E1 and to Ca_2E1P: bold line, the spectrum of ADP binding to Ca_2E1P (*shaded* spectrum minus *thin line* spectrum in *panel A*); thin line, the spectrum of ADP binding to Ca_2E1, normalized to the same amplitude as the bold spectrum of ADP binding to Ca_2E1P. (*C*) Time courses of band areas at 1628 (Liu and Barth, 2004) and 1720 cm^{-1} in the presence and absence of apyrase obtained with 3 mM ATP and 1.2 mM Ca^{2+}-ATPase. The time constants for the 1628 cm^{-1} band are $t_1 = 0.1$ s, $t_2 = 16$ s. The 1720 cm^{-1} band decayed with a half time of more than 10 min. Time constants and lines were obtained by fitting data with first or second order exponential decay functions.

C. The data were fitted with two time constants, one for ATP binding to the Ca^{2+}-ATPase (0.1 s) and the other for ADP splitting by apyrase (16 s). Under our conditions, the apyrase reaction with ADP, which is generated from ATP hydrolysis by the Ca^{2+}-ATPase, is slower than ATPase phosphorylation but faster than the decay of Ca_2E1P. The decay of Ca_2E1P was observed with the marker bands of phosphorylation at 1720 and 1549 cm^{-1}. The band amplitudes decreased very slowly with a half time of more than 10 min.

In summary, the phosphoenzyme obtained in the first 5 s was Ca_2E1P with bound ADP, which was generated from ATP hydrolysis by the Ca^{2+}-ATPase. In the presence of apyrase, ADP that dissociated from Ca_2E1P was hydrolyzed by apyrase. The black bold spectrum shown in Fig. 9 *B* was obtained by subtraction between the spectra obtained before and after ADP dissociation from Ca_2E1P. It reflects ADP binding to Ca_2E1P and is a mirror image of the ADP dissociation spectrum. It is very similar in shape to the spectrum of ADP binding Ca_2E1 (*thin* spectrum in Fig. 9 *B*, multiplied with a factor of 0.42 to have the same band amplitudes in the amide I region; Barth et al., 1994; Liu and Barth, 2002). This indicates that ADP dissociation results in conformational changes, which are the reverse of those induced by ADP binding to the ATPase. However, the extent of these changes seems to be smaller when ADP dissociates from Ca_2E1P, since the associated amplitudes of infrared bands in the amide I region are only ~40% of those of ADP binding.

DISCUSSION

Infrared characterization of the enzymatic reactions of AdK and apyrase

Both AdK and apyrase can be used as helper enzymes to remove ADP generated after ATP hydrolysis in our ATPase experiments under suitable conditions. The concentration of helper enzymes could be kept low enough not to cause observable changes in their infrared absorption. Thus, the protein of interest could be observed nearly without disturbing overlapping infrared bands that arise from the helper enzymes. Only below 1300 cm^{-1} the spectra reveal the change in nucleotide concentration catalyzed by them. We characterized the difference spectra associated with their enzymatic reactions, which can be used to assess their function and to relate kinetics of the protein of interest to helper enzyme activity. In general, the measurement of enzyme activity will be an important future application of infrared spectroscopy because it provides a direct observation of substrates and products, and therefore does not require the development of an activity assay. Our work adds two more items to the growing list of enzymatic reactions

that have been monitored by infrared spectroscopy (see for example Fisher et al., 1980; Jencks, 1963; Karmali et al., 2004; Pacheco et al., 2003; Thoenges and Barth, 2002; White et al., 1992).

Both helper enzymes remove ADP from our samples with the benefit that the photolysis experiment can be repeated several times without the inhibiting influence of ADP. In addition each helper enzyme has its particular advantages, and the particular choice will depend on the purpose of the experiment.

AdK applied to experiments with ATP and the Ca^{2+}-ATPase

Helper enzymes should be used under conditions where they do not disturb the reactions of interest. In our experiments with AdK (1 mg/ml AdK, 1°C), the AdK reaction is slow with a time constant of 32 s in the absence of ATPase (Fig. 2) and of 17 s in the presence of ATPase (Fig. 4). In our ATP release experiments with the Ca^{2+}-ATPase, the accumulation of Ca_2E1P is fast (~2 s with ATP, in the presence and absence of AdK; Liu and Barth, 2003a) and has little overlap with the slow AdK reaction. This reaction is therefore not affected by the presence of AdK. AdK was used in ATPase samples to enable repetition of the ATP-release experiment on the same sample. Without AdK, the reaction products of the ATPase reaction, ADP, inhibits reactions of ATP generated in subsequent flashes. In our measurements with ATPase and AdK, samples were kept at room temperature for 1 h after ATP release to equilibrate. The newly formed ATP in the AdK reaction was hydrolyzed and consumed by the ATPase during the equilibration time. The ATPase returned thereafter into the initial Ca_2E1 state. Such samples can be flashed several times (usually up to four times) without the interference by ADP (Barth et al., 1996). The final reaction product of the AdK reaction in our samples, AMP, will not affect ATPase partial reactions because of the low affinity of ATPase to AMP (Lacapere et al., 1990; Liu and Barth, 2003a).

An ongoing study at our laboratory indicates that AdK can also be used as a helper enzyme to achieve an isotopic exchange in nucleotides, as has been observed for ADK (Dale and Hackney, 1987; Dawson et al., 1985), as well as other enzymes (Rose, 1979), and used for the synthesis of isotopically labeled nucleotides (see, for example, Dawson et al., 1985; Webb and Trentham, 1980). The particular aim of our approach is to induce a ^{16}O to ^{18}O isotope exchange at the oxygen atoms of the phosphate group transiently bound to the Ca^{2+} ATPase in the Ca_2E1P and E2P states by using isotopically labeled ATP. The ATPase is first phosphorylated with ATP labeled at the β-phosphate, resulting in phosphoenzyme with unlabeled phosphate. With the help of AdK, ADP produced from ATP hydrolysis is converted into ATP again. The generated ATP, now labeled at the β- and γ-phosphate, phosphorylates the ATPase and produces labeled phosphoenzyme (unpublished data). Difference spectra of the isotope exchange will make it possible to determine vibrational frequencies of the phosphoenzyme phosphate. This approach of achieving an isotope exchange within one sample generates difference spectra of higher sensitivity because differences between samples are avoided (Barth, 2002).

ADP dissociation from Ca_2E1P

Apyrase served well in our application as a helper enzyme. By removing ADP from samples accumulating Ca_2E1P, we find that ADP plays an important role for the conformation of Ca_2E1P (Liu and Barth, 2004). This we infer from the shape of the spectrum of ADP binding to Ca_2E1P shown in Fig. 9. It is very similar in shape to that of ADP binding to Ca_2E1, which is similar to that of ATP binding (Liu and Barth, 2002). From the similarity in shape we conclude that ADP binding to Ca_2E1P produces a conformational change that is similar in character to that of ATP binding to Ca_2E1 but smaller in extent. Since ATP binding induces the transition between an open conformation of the cytoplasmic domains to a closed conformation (Sorensen et al., 2004; Toyoshima and Mizutani, 2004), we conclude that ADP binding to Ca_2E1P induces part of this transition or, in other words, that ADP dissociation from Ca_2E1P relaxes the closed conformation of Ca_2E1P with ADP bound (Ca_2E1P:ADP) partially back to the open conformation of Ca_2E1. An additional finding is that ADP dissociation from Ca_2E1P does not trigger the transition to E2P, since the spectral characteristics of E2P (Barth et al., 1994, 1996; Barth, 1999) are not observed upon ADP dissociation. A further discussion of the infrared signals of conformational change upon nucleotide binding can be found in our previous publications (Barth and Zscherp, 2000; Liu and Barth, 2003a, 2004).

Evaluation of the use of AdK and apyrase as helper enzymes

The rate of removal of ADP by AdK can be adjusted by varying the AdK concentration, temperature, and pH value, depending on the purpose of the experiment. A further effect of AdK is to maintain the presence of ATP for a longer time without photolyzing more caged ATP, which would increase the photolysis signals. However, the presence of ATP, ADP, and AMP in the same sample makes reaction kinetics more complicated, and caution is needed in the interpretation of kinetics and of spectra in the region of phosphate absorption. For example, a faster apparent rate of ATP hydrolysis by the Ca^{2+}-ATPase is observed in the absence of AdK than in its presence because of ATP regeneration by ADK (Liu and Barth, 2004).

Precaution is required in the application of apyrase because it also reacts with ATP. There is competition between ATPase and apyrase for ATP after ATP release

from caged ATP. In the presence of apyrase, the ATP concentration available for the ATPase is less than that in the absence of apyrase. Furthermore, P_i from splitting of ATP and of ADP by apyrase is at twice the concentration of that produced from ATP hydrolysis by the ATPase. Such conditions help accumulate the E2P state, if this state is the one of interest. The choice whether to use AdK or apyrase will depend on the particular experiment. Apyrase has the advantage of removing ADP without generating ATP but also cleaves ATP, which is used to trigger the initial enzyme reaction. AdK is probably preferable when resynthesis of ATP, and in consequence reinitiation of the enzymatic reaction, is not a problem.

Perspectives on the use of helper enzymes

For other nucleotides, these or other helper enzymes or enzyme systems can be used to remove nucleoside diphosphate or regenerate nucleotides, such as pyruvate kinase/phosphoenolpyruvate (Too et al., 1989) or polyphosphate kinase/polyphosphate-AMP phosphotransferase (Kameda et al., 2001) to regenerate GTP from GDP or GMP, guanylate kinase to generate GTP from GDP, and thymidylate kinase to generate TTP from TDP. A complementary application of helper enzymes is their use to generate a compound of interest from a precursor that is released by flash photolysis. This widens the application range of caged compounds in cases where an appropriate caged compound cannot be used directly because it is not available or reacts with or binds to the enzyme despite the caging group. Related to this is the above-mentioned change in isotopic composition of a substrate catalyzed by AdK.

The authors thank J. E. T. Corrie (National Institute for Medical Research, London) for the preparation of caged compounds and W. Hasselbach (Max-Planck-Institut, Heidelberg, Germany) for the gift of Ca^{2+}-ATPase.

This work was supported by Vetenskapsrådet, Knut och Alice Wallenbergs Stiftelse, and Stockholm Graduate School of Molecular Life Sciences.

REFERENCES

Atkinson, D. E. 1968. The energy charge of adenylate pool as a regulatory parameter. *Biochemistry.* 7:4030–4034.

Barth, A. 1999. Phosphoenzyme conversion of the sarcoplasmic reticulum Ca^{2+}-ATPase. Molecular interpretation of infrared difference spectra. *J. Biol. Chem.* 274:22170–22175.

Barth, A. 2002. Selective monitoring of 3 our of 50,000 protein vibrations. *Biospectroscopy.* 67:237–241.

Barth, A., K. Hauser, W. Mäntele, J. E. T. Corrie, and D. R. Trentham. 1995. Photochemical release of ATP from 'caged ATP' studied by time-resolved infrared spectroscopy. *J. Am. Chem. Soc.* 117:10311–10316.

Barth, A., W. Kreutz, and W. Mantele. 1994. Changes of protein structure, nucleotide microenvironment, and Ca^{2+} binding states in the catalytic cycle of sarcoplasmic reticulum Ca^{2+}-ATPase: investigation of nucleotide binding, phosphorylation and phosphoenzyme conversion by FTIR difference spectroscopy. *Biochim. Biophys. Acta.* 1194:75–91.

Barth, A., and W. Mäntele. 1998. ATP-induced phosphorylation of the sarcoplasmic reticulum Ca^{2+}-ATPase—molecular interpretation of infrared difference spectra. *Biophys. J.* 75:538–544.

Barth, A., W. Mäntele, and W. Kreutz. 1990. Molecular changes in the sarcoplasmic reticulum Ca^{2+}-ATPase during catalytic activity. A Fourier transform infrared (FTIR) study using photolysis of caged ATP to trigger the reaction cycle. *FEBS Lett.* 277:147–150.

Barth, A., F. von Germar, W. Kreutz, and W. Mäntele. 1996. Time-resolved infrared spectroscopy of the Ca^{2+}-ATPase. The enzyme at work. *J. Biol. Chem.* 271:30637–30646.

Barth, A., and C. Zscherp. 2000. Substrate binding and enzyme function investigated by infrared spectroscopy. *FEBS Lett.* 477:151–156.

Barth, A., and C. Zscherp. 2002. What vibrations tell us about proteins. *Q. Rev. Biophys.* 35:369–430.

Brintzinger, H. 1965. Intrasphärische und extrasphärische Komplexe mit Phosphatliganden, Infrarotspektren von Phosphatkomplexen in wässeriger Lösung. *Helv. Chim. Acta.* 48:47–54.

Buchet, R., I. Jona, and A. Martonosi. 1991. Ca^{2+} release from caged-Ca^{2+} alters the FTIR spectrum of sarcoplasmic reticulum. *Biochim. Biophys. Acta.* 1069:209–217.

Cepus, V., A. J. Scheidig, R. S. Goody, and K. Gerwert. 1998a. Time-resolved FTIR studies of the GTPase reaction of H-ras p21 reveal a key role for the β-phosphate. *Biochemistry.* 37:10263–10271.

Cepus, V., C. Ulbrich, C. Allin, A. Troullier, and K. Gerwert. 1998b. Fourier transform infrared photolysis studies of caged compounds. *Methods Enzymol.* 291:223–245.

Dale, M. P., and D. D. Hackney. 1987. Analysis of positional isotope exchange in ATP by cleavage of the βP-OγP bond demonstration of negligible positional isotope exchange by myosin. *Biochemistry.* 26: 8365–8372.

Dawson, J. M., N. D. Cook, and T. J. Peters. 1985. Enzymatic synthesis of [β-^{32}P] ADP using adenylate kinase and [γ-^{32}P] ATP. *Anal. Biochem.* 149:471–473.

Du, X., H. Frei, and S. H. Kim. 2000. The mechanism of GTP hydrolysis by Ras probed by Fourier transform infrared spectroscopy. *J. Biol. Chem.* 275:8492–8500.

Epp, A., T. Ramasarma, and L. R. Wetter. 1958. Infrared studies on complexes of Mg2+ with adenosine phosphates. *J. Am. Chem. Soc.* 80:724–727.

Fisher, J., J. G. Belasco, S. Khosla, and J. R. Knowles. 1980. β-Lactamase proceeds via an acyl-enzyme intermediate. Interaction of the Escherichia coli RTEM enzyme with cefoxitin. *Biochemistry.* 19:2895–2901.

Hasselbach, W., and M. Makinose. 1961. Die Calciumpumpe der ''Erschlaffungsgrana'' des Muskels und ihre Abhängigkeit von der ATP-Spaltung. *Biochem. Z.* 333:518–528.

Inesi, G., H. Ma, D. Lewis, and C. Xu. 2004. Ca^{2+} occlusion and gating function of Glu309 in the ADP-fluoroaluminate analog of the Ca^{2+}-ATPase phosphoenzyme intermediate. *J. Biol. Chem.* 279:31629–31637.

Jencks, W. P. 1963. Infrared measurements in aqueous media. *Methods Enzymol.* 6:914–928.

Kalckar, H. M. 1944. Adenylpyrophosphatase and myokinase. *J. Biol. Chem.* 153:355–367.

Kameda, A., T. Shiba, Y. Kawayoe, Y. Satoh, Y. Ihara, M. Munekata, K. Ishige, and T. Noguchi. 2001. A novel ATP regeneration system using polyphosphate-AMP phosphotransferase and polyphosphate kinase. *J. Biosci. and Bioeng.* 91:557–563.

Kaplan, J. H., B. Forbush, and J. F. Hoffman. 1978. Rapid photolytic release of ATP from a protected analogue: utilization by the Na:K pump of human red blood cell ghosts. *Biochemistry.* 17:1929–1935.

Karmali, K., A. Karmali, A. Teixeira, and M. J. M. Curto. 2004. The use of Fourier transform infrared spectroscopy to assay for urease from Pseudomonas aeruginosa and Canavalia ensiformis. *Anal. Biochem.* 331:115–121.

Komosyznski, M., and A. Wojtczak. 1996. Apyrase (ATP diphosphohydrolases, EC 3.6.1.5): function and relationship to ATPases. *Biochim. Biophys. Acta.* 1310:233–241.

Lacapere, J.-J., N. Bennett, Y. Dupont, and F. Guillain. 1990. pH and Magnesium dependence of ATP binding to SR ATPase. *J. Biol. Chem.* 265:348–353.

Ladner, W. E., and G. M. Whitesides. 1985. Enzymatic synthesis of deoxyATP using DNA as starting material. *J. Org. Chem.* 50:1076–1079.

Lee, A., and J. East. 2001. What the structure of a calcium pump tells us about its mechanism. *Biochem. J.* 356:665–683.

Liu, M., and A. Barth. 2002. Mapping nucleotide binding site of calcium ATPase with IR spectroscopy: effects of ATP gamma-phosphate binding. *Biospectroscopy.* 67:267–270.

Liu, M., and A. Barth. 2003a. Mapping interactions between the Ca^{2+}-ATPase and its substrate ATP with infrared spectroscopy. *J. Biol. Chem.* 278:10112–10118.

Liu, M., and A. Barth. 2003b. TNP-AMP binding to the sarcoplasmic reticulum Ca^{2+}-ATPase studied by infrared spectroscopy. *Biophys. J.* 85:3262–3270.

Liu, M., and A. Barth. 2004. Phosphorylation of the sarcoplasmic reticulum Ca^{2+}-ATPase from ATP and ATP analogs studied by infrared spectroscopy. *J. Biol. Chem.* In press.

Lu, Q., and M. Lnouye. 1996. Adenylate kinase complements nucleoside diphosphate kinase deficiency in nucleotide metabolism. *Proc. Natl. Acad. Sci. USA.* 93:5720–5725.

MacLennan, D. H., and N. M. Green. 2000. Pumping Ions. *Nature.* 405:633–634.

Mäntele, W. 1993. Reaction-induced infrared difference spectroscopy for the study of protein function and reaction mechanisms. *Trends Biochem. Sci.* 18:197–202.

Mäntele, W. 1996. Infrared and Fourier-transform infrared spectroscopy. *In* Biophysical Techniques in Photosynthesis. J. Amesz and A. J. Hoff, editors. Kluwer Academic Publishers, Dordrecht, The Netherlands. 137–160.

Martonosi, A. N., and S. Pikula. 2003. The structure of the Ca^{2+}-ATPase of sarcoplasmic reticulum. *Acta Biochim. Pol.* 50:337–365.

Meyerhof, O. 1945. The origin of the reaction of harden and young in cell-free alcoholic fermentation. *J. Biol. Chem.* 157:105–119.

Pacheco, R., M. L. M. Serralheiro, A. Karmali, and P. I. Haris. 2003. Measuring enzymatic activity of a recombinant amidase using Fourier transform infrared spectroscopy. *Anal. Biochem.* 322:208–214.

Plow, E. F., and G. A. Marguerie. 1980. Induction of the fibrinogen receptor on human platelets by epinephrine and the combination of epinephrine and ADP. *J. Biol. Chem.* 255:10971–10977.

Raimbault, C., R. Buchet, and C. Vial. 1996. Changes of creatine kinase secondary structure induced by the release of nucleotides from caged compounds—an infrared difference-spectroscopy study. *Eur. J. Biochem.* 240:134–142.

Resnick, S. M., and A. J. B. Zehnder. 2000. In vitro ATP regeneration from polyphosphate and AMP by polyphosphate: AMP phosphotransferase and adenylate kinase from Acinetobacter johnsonii 210A. *Appl. Environ. Microbiol.* 66:2045–2051.

Rose, I. A. 1979. Positional isotope exchange studies of enzyme mechanisms. *Adv. Enzymol. Relat. Areas Mol. Biol.* 50:361–395.

Shimanouchi, T., M. Tsuboi, and Y. Kyogoku. 1964. Infrared spectra of nucleic acids. *In* Advances in Chemical Physics. J. Duchesne, editor. Wiley Interscience, New York. 435–498.

Siebert, F. 1995. Infrared spectroscopy applied to biochemical and biological problems. *Methods Enzymol.* 246:501–526.

Sorensen, T. L.-M., J. V. Moller, and P. Nissen. 2004. Phosphoryl transfer and calcium ion occlusion in the calcium pump. *Science.* 304:1672–1675.

Stokes, D. L., and N. M. Green. 2003. Structure and function of the calcium pump. *Annu. Rev. Biophys. Biomol. Struct.* 32:445–468.

Straub, F. B., and G. Feuer. 1950. Adenosinetriphosphate. The functional group of actin. *Biochim. Biophys. Acta.* 4:455–470.

Takeuchi, H., H. Murata, and I. Harada. 1988. Interaction of adenosine 5'-triphosphate with Mg^{2+}: vibrational study of coordination sites by use of ^{18}O-labeled triphosphates. *J. Am. Chem. Soc.* 110:392–397.

Thoenges, D., and A. Barth. 2002. Direct measurement of enzyme activity with infrared spectroscopy. *J. Biomol. Screen.* 7:353–357.

Too, C. K., P. R. Murphy, and H. G. Friesen. 1989. G-proteins modulate prolactin- and interleukin-2-stimulated mitogenesis in rat Nb2 lymphoma cells. *Endocrinology.* 124:2185–2192.

Toyoshima, C., and G. Inesi. 2004. Structural basis of ion pumping by Ca^{2+}-ATPase of the sarcoplasmic reticulum. *Annu. Rev. Biochem.* 73: 269–292.

Toyoshima, C., and T. Mizutani. 2004. Crystal structure of the calcium pump with a bound ATP analogue. *Nature.* 430:529–535.

Toyoshima, C., M. Nakasako, H. Nomura, and H. Ogawa. 2000. Crystal structure of the calcium pump of sarcoplasmic reticulum at 2.6 Å resolution. *Nature.* 405:647–655.

Troullier, A., K. Gerwert, and Y. Dupont. 1996. A time-resolved Fourier transformed infrared difference spectroscopy study of the sarcoplasmic reticulum Ca^{2+}-ATPase: kinetics of the high-affinity calcium binding at low temperature. *Biophys. J.* 71:2970–2983.

von Germar, F., A. Barth, and W. Mäntele. 2000. Structural changes of the sarcoplasmic reticulum Ca^{2+} ATPase upon nucleotide binding studied by Fourier transform infrared spectroscopy. *Biophys. J.* 78:1531–1540.

von Germar, F., A. Galan, O. Llorca, J. L. Carrascosa, J. M. Valpuesta, W. Mäntele, and A. Muga. 1999. Conformational changes generated in GroEL during ATP hydrolysis as seen by time-resolved infrared spectroscopy. *J. Biol. Chem.* 274:5508–5513.

Wang, J. H., D. G. Xiao, H. Deng, R. Callender, and M. R. Webb. 1998. Vibrational study of phosphate modes of GDP and GTP and their interaction with magnesium in aqueous solution. *Biospectroscopy.* 4: 219–227.

Webb, M. R., and D. R. Trentham. 1980. Analysis of chiral inorganic [^{16}O, ^{17}O, ^{18}O]thiophosphate and the stereochemistry of the 3-phosphoglycerate kinase reaction. *J. Biol. Chem.* 255:1775–1779.

West, J. J., B. Nagy, and J. Gergely. 1967. Free adenosine diphosphate as an intermediary in the phosphorylation by creatine phosphate of adenosine diphosphate bound to actin. *J. Biol. Chem.* 242:1140–1145.

White, A. J., K. Drabble, S. Ward, and C. W. Wharton. 1992. Analysis and elimination of protein perturbation in infrared difference spectra of acyl-chymotrypsin ester carbonyl groups by using ^{13}C isotopic substitution. *Biochem. J.* 287:317–323.

Whitesides, G. M., A. Lamotte, O. Adalsteinsson, and C. K. Colton. 1976. Covalent immobilization of adenylate kinase and acetate kinase in a polyacrylamide gel: enzymes for ATP regeneration. *Methods Enzymol.* 44:887–897.